Talens Oliag, P.; Castells, ML.; Verdú, S.; Barat Baviera, JM.; Grau Meló, R. (2021). Flow, viscoelastic and masticatory properties of tailor made thickened pea cream for people with swallowing problems. Journal of Food Engineering. 292:1-10. https://doi.org/10.1016/j.jfoodeng.2020.110265

Flow, viscoelastic and masticatory properties of tailor made thickened pea cream for people with swallowing problems

Talens, P[*1]; Castells, M. L[1,2].; Verdú, S[1]; Barat, J.M. [1]; Grau, R. [1]

1. Departamento de Tecnología de Alimentos. Universitat Politècnica de València. Camino de Vera s/n, 46022 Valencia (Spain).

2. Departamento de Desarrollo de Procesos. Subgerencia Operativa de Tecnología de Alimentos. Instituto Nacional de Tecnología Industrial. Avenida General Paz 5445, 1650 San Martin, Buenos Aires (Argentina)

*Corresponding author:

Pau Talens Oliag; e-mail: pautalens@tal.upv.es

ABSTRACT

This study evaluated the flow, viscoelastic and masticatory properties of tailor made pea cream using different hydrocolloids, and the potential effect that saliva could have while chewing. The creams thickened with pectin, carboxymethyl cellulose, tara gum and konjac gum showed the weakest internal gel structure with highest values of loss tangent at 1Hz (0.49±0.07), slope of log elastic modulus *versus* log frequency (0.34±0.05) and maximum capacitance (0.07±0.02 Pa^{-1}). The samples thickened with commercial hydrocolloids were affected the most by the presence of saliva, with a significant reduction in apparent viscosity at 10 s^{-1}, that ranged from 1500 mPas until 11000 mPas. These results demonstrate that it is possible to optimize the structure of thickened pea cream for dysphagia by using, for example, carboxymethyl cellulose, tara

gum and konjac gum, because they provide a greater viscous component, and, therefore, a bolus that is more easy to swallow.

Keywords: dysphagia; rheology; creep recovery; oscillatory test; thickeners; saliva.

1. Introduction

Dysphagia, or the difficulty to swallow regular food and liquids safely and effectively, affects about 8% of the world's population (Cichero et al., 2013). Patients with dysphagia find thin liquids through the pharynx difficult to control, which may lead to choking, aspiration, pneumonia, and even death (Martino et al., 2005). The main strategy to treat this problem is using thickeners to obtain texture-modified foods and thickened fluids, which allow a slightly more cohesive bolus to form that makes swallowing slower and safe (Cichero, 2013, Nishinari et al., 2016). However, over-thickened foods can lead to long transit times and can leave residue inside the pharynx, which may incur aspiration risk (Cichero & Murdoch, 2006). The type of employed thickener has been shown to contribute to aspiration risk to a greater or lesser extent (Leonard, et al., 2014.).

The most accepted dysphagia guide (National Dysphagia Diet, 2002) classifies these foods according to their shear viscosity at a shear rate of 50 s^{-1} at 25ºC, at the following levels: thin (1-50 mPas); nectar-thick (50-350 mPas); honey-thick (350-1750 mPas); pudding-thick (> 1750 mPas) (Gallegos et al., 2012; Cichero et al., 2013). However, this classification does not consider any other relevant factors that affect liquid flow such as density, sample temperature, yield stress, the wide range of shear rates that occur during the swallowing process, bolus viscoelasticity, and propulsion pressure (Cichero et al., 2017). Furthermore, thickened fluids are non-Newtonian fluids, so it is impossible to fully characterise them only with viscosity measurements. Texture-modified food obtained with different thickening agents may have the same apparent viscosity at the indicated temperature and shear rate, but exhibit different flow behaviours and distinct viscoelastic and mechanical properties.

Selecting an adequate thickener to obtain texture-modified foods is essential to ensure safe swallowing in dysphagia patients. Most authors have focused on studying the effect of different variables (pH, time, temperature, etc.) on the rheological behaviour of texture-modified food (Zargaraan et al., 2013; Abu-Zarim, Zainul-Abidin & Ariffin, 2018). Some authors have also evaluated viscoelastic behaviour (Mackley et al., 2013; Moret-Tatay et al., 2015), but very few studies have studied rheological, viscoelastic, and masticatory behaviours at the same time using different thickeners on various food matrices at several thick levels. Sharma, Kristo, Corredig, & Duizer (2017), studied these behaviours in mashed carrots thickened at the pudding-thick level, but no studies were found for thickened pea creams.

Furthermore, saliva plays a very important role in oral processing and bolus rheology because it facilitates the swallowing process by lubricating the mouth and helping to form a cohesive bolus (Boehm et al., 2019). Mucins mainly decrease friction in the mouth by making smooth the bolus movement from the oral phase to the pharynx (Chen, 2009). The bolus must also move through the pharynx at an adequate speed and must be structurally homogeneous to be transferred as a "mass", which is key for easy swallowing (Ishihara et al., 2011). In addition, saliva's complex composition can produce changes in the physical properties of some hydrocolloids, especially those based on starch, by reducing, for example, its viscosity (Hanson et al., 2012a; Hanson et al., 2012b).

This paper is focused on the study of the flow, viscoelastic and masticatory properties of a tailor made food for people with swallowing problems. Understanding these properties is an advantage in designing better controlled fluids that are critically important in influencing bolus flow and swallowing. Specifically, the work analyses tailor made thickened pea cream at two levels (honey-thick and pudding-thick) using 10

hydrocolloids including 2 specific commercial thickeners for dysphagia. The potential effect that saliva could have while chewing is also evaluated.

2. Materials and Methods

Pea cream was prepared with green peas, olive oil, salt, and water. All ingredients were purchased from a local supermarket (Valencia, Spain). In order to obtain a wide range of thickeners, in this study eight hydrocolloids and two commercial dysphagia-specific thickener products were selected. Xanthan gum (XG), high methoxyl pectin (HMP), Guar gum (GG), carragenate (C), and sodium carboxymethylcellulose (CMC) were provided by EPSA, Valencia, Spain. Gellan gum (GEG), Konjac gum (KG) and Tara gum (TG) were purchased from Cocinista, Madrid, Spain. Nutilis® (NI) (ingredients: modified wazy maize starch, guar gum, xanthan gum, tara gum, maltodextrin and E1442: hydroxypropyl distarch phosphate) and Nutavant® (NA) (ingredients: modified maize starch) were purchased from a local pharmacy.

α-amylase from porcine pancreas Type VI-B (13 $U \cdot mg^{-1}$) and mucin from porcine stomach Type II were purchased from Sigma-Aldrich. Potassium citrate, potassium chloride (>99%), potassium phosphate (>99%), ammonium nitrate, uric acid sodium salt, sodium DL-lactate (99% and 112.06 g/mol), urea (99.5%) and sodium chloride were of analytical certified grade. The employed water was deionised.

2.1. Sample preparation

Pea cream was prepared in a Thermomix® (TM31, Wuppertal, Germany). Green peas were cooked with olive oil, water and salt. Tailor made pea-thickened samples were prepared 24 h before testing by adding hydrocolloids to the pea cream. Cream was stirred by a magnetic stirrer for 30 minutes to achieve uniform dispersion. After

preparing samples, they were refrigerated at 5ºC until tests. Two independent batches were prepared for all the samples. The pea cream apparent viscosity determined at a shear rate of 50 s^{-1} and 25ºC was 299±33 mPas (nectar-thick level). The concentration of each hydrocolloid added to the pea cream was determined to obtain an apparent viscosity, at a shear rate of 50 s^{-1} measured at 25ºC, close to 1500 mPas (honey-thick level) and 4100 mPas (pudding-thick level). Table 1 shows the concentrations of each hydrocolloid and the resulting pea creams viscosities.

2.2. Preparing artificial saliva

Artificial saliva was prepared according to the composition employed in the previous studies by Chung et al. (2012) and Torres et al. (2019) using 3% mucin and α-amylase with an activity of 93 $U \cdot mL^{-1}$.

2.3. Flow and viscoelastic characterisation

Flow and viscoelastic characterisation was performed in a Kinexus Pro+ Rheometer (Malvern Instruments Ltd., MA, USA) equipped with a parallel plate geometry (PLC61/PU40). The rheometer came with a Peltier heating system for accurate temperature control. Samples were loaded onto the lower plate surface, and the upper plate was lowered until it reached a gap of 1 mm. After loading, all the samples were held for a 5-minute resting time in the measuring geometry before testing to allow stress relaxation and temperature equilibration. Each measurement was performed in triplicate and measured at 25ºC. The flow rheological properties and the non-linear and linear viscoelastic behaviours of all the samples were studied.

2.3.1. Flow rheological properties

The flow rheological properties of both pea cream and thickened pea creams were characterised by analysing both transient and steady flow behaviours.

Transient flow behaviour was analysed by hysteresis experiments, which consisted of a three-step operation: upstream curve, plateau curve, downstream curve. An increasing shear rate ramp, ranging from 0.01 s^{-1} to 100 s^{-1} in 5 minutes, was set to measure the upstream curve. The plateau curve was obtained at a constant shear rate of 100 s^{-1} for 5 minutes. The shear rate ramp, ranging from 100 s^{-1} to 0.01 s^{-1} in 5 minutes, was set to measure the downstream curve. For all the samples, the areas under the upstream data points (Aup) and the areas under the downstream data points (Adown), as well as the percentage of relative hysteresis area Ar = (Aup – Adown) /Aup x 100), were calculated (Dolz et al., 2000; Tárrega et al., 2004).

The viscous flow behaviour samples were analysed after eliminating flow time dependence, and applying a previous 5-minute shearing time at 100 s^{-1} by steady shear rheological experiments. Flow curves were obtained using increasing shear rates from 0.1 to 100 s^{-1} for 5 minutes. The obtained data was fitted to the Ostwald-de Wale (power-law) model (Equation 1).

$$\sigma = K \cdot \dot{\gamma}^{n} \quad (1)$$

where σ is shear stress (Pa), $\dot{\gamma}$ is the shear rate (s^{-1}), K is the consistency coefficient ($Pa \cdot s^{n}$) and n is the flow behaviour index (dimensionless). Goodness-of-fit was evaluated by correlation coefficient R^2.

2.3.2. Viscoelastic analysis

The viscoelastic properties of the samples were characterised by non-linear and linear viscoelastic analyses. Two large amplitude oscillatory shear (LAOS) tests, namely a

153 strain sweep test and a stress sweep test, were performed to characterise the non-linear
154 viscoelastic properties, and to determine the limits of the linear viscoelastic region
155 (LVR). The strain sweep test was conducted at a frequency of 1 Hz within a strain range
156 of 0.01 and 100%. The stress sweep test was run at a frequency of 1 Hz within a stress
157 range of 0.01 and 100 Pa for the honey-thick samples, and one of 0.1 and 200 Pa for the
158 pudding-thick samples. The linear viscoelastic properties of the samples were
159 characterised by a small amplitude oscillatory shear test and a creep-recovery test. The
160 small amplitude oscillatory shear (SAOS) test was performed from 0.1 to 100 Hz at
161 0.1% strain for the honey-thick samples and at 0.2% strain for the pudding-thick
162 samples. The creep recovery test was carried out by subjecting samples to a constant
163 stress value at LVR during 5 minutes, followed by 5 minutes recovering decreasing
164 stress to zero.
165 For the LAOS tests, the changes in elastic modulus (G', Pa) and viscous modulus (G'',
166 Pa) with strain (strain sweep test) and stress (stress sweep test) were recorded. The
167 elastic modulus value at LVR (G'_{LVR}), the strain value at LVR ($Strain_{LVR}$), the stress
168 value at LVR ($Stress_{LVR}$) and the flow point were also recorded.
169 For the SAOS tests, the changes in elastic modulus (G´, Pa), viscous modulus (G´´, Pa),
170 complex modulus (G*, Pa), complex viscosity (η*, Pa), phase angle (δ, º) and loss
171 tangent (Tan δ = G"/G', dimensionless) were recorded.
172 The results of the creep-recovery tests were described in terms of capacitance (J (t) Pa^{-1}),
173 the ratio between deformation (%) and applied stress (Pa).
174

175 **2.4. Mastication assay**

176 To simulate oral chewing, the instrumental mastication assay developed by Chung et al.
177 (2012) was performed by a Kinexus Pro+ Rheometer (Malvern Instruments Ltd., MA,

178 USA). Food samples were compressed, subjected to a constant shear rate, and
179 decompressed for a number of cycles to simulate the movement of both tongue and
180 palate in the semisolid food chewing stage. The thickened pea creams were
181 characterised using a 10-cycle chewing sequence at 37ºC. To evaluate the effect of
182 saliva on the rheological properties, the test was run in the absence and presence of
183 saliva by adding 0.2 mL of artificial saliva to samples. All measurements were made in
184 triplicate.
185
186 **2.5. Statistical analysis**
187 A statistical data analysis was performed by an analysis of variance (ANOVA) using the
188 Statgraphics Centurion XVII.II-X64 programme (Statgraphics Technologies Inc.,
189 Virginia, USA). Fisher's least significant difference (LSD) was used at the 95%
190 confidence level.
191
192 **3. Results and Discussion**
193 **3.1. Flow rheological and viscoelastic characterisation**
194 The flow rheological, non-linear and linear viscoelastic behaviour of all the samples
195 were studied. For the flow rheological properties and non-linear viscoelastic analysis,
196 major deformations were applied to samples to define material behaviour under flow.
197 For the linear viscoelastic analysis, minor deformations were applied to samples to
198 establish the representative parameters of the material's original microstructure.
199 **3.1.1. Flow rheological analysis**
200 The transient flow behaviour analysis showed that both the pea cream and thickened pea
201 creams exhibited thixotropic time-dependent behaviour, which means that viscosity
202 values decreased with shearing time. As samples had different viscosities, time-

dependent behaviour was analysed by the percentage of relative hysteresis area (Ar) (Dolz et al., 2000). This Ar is an index of the energy needed to destroy the sample's inner structure, which is responsible for the impact of time on flow behaviour. Higher Ar values would suggest a more intense destruction of sample inner structure (Jiang et al., 2015; Alvarez et al., 2017). The Ar percentage of the pea cream was 26.4±1.2%. The Ar percentages of all the thickened samples are shown in Table 2. The Ar percentage was higher in the pea cream than in the thickened pea creams, which indicated that the pea cream needed more energy to break down the structure. The addition of a thickener implies less damage to the inner pea cream structure. This damage is less when the thickener concentration is higher (pea creams at the pudding-thick level) than when it is lower (pea creams at the honey-thick level). Of all the studied thickeners, GG seemed the be the best hydrocolloid to maintain the product's internal structure with the imposed shear time, followed by TG and GEG in pea creams at the honey-thick level, and by TG, KG and CMC in pea creams at the pudding-thick level.

Steady flow behaviour was measured after reducing the flow time dependence by shearing. A typical flow curve for the pea cream and thickened pea cream is shown in Figure 1. All the samples clearly exhibited shear-thinning flow behaviour. Sample viscous flow behaviour was described by the Ostwald-de Waele (power law) model. The parameters obtained for the power law model are summarised in Table 2. The obtained good correlation coefficients, R^2, indicated that the model would be suitable for describing the rheology of both pea cream and thickened pea creams. The flow behaviour indices (n) were less than unity, as expected with non-Newtonian shear-thinning behaviour. The thickened pea samples showed the most pseudoplastic properties, and pea creams at the pudding-thick level had the lowest flow behaviour

indices, corresponding to the highest shear stress values obtained for these samples (Figure 1).

The mean n values in the power law model for the samples at the honey-thick level (0.34±0.07) were slightly higher than for the samples at the pudding-thick level (0.25±0.09), and were similar to other products like tomato puree, pimento puree, carrot puree and vegetable-based infant puree (Okechukwu & Rao, 1999; Cepeda et al., 2000; Van Hecke et al., 2012; Alvarez & Canet, 2013).

As expected, the lowest consistency coefficient (K) values corresponded to the samples at the nectar-thick level (2.7±0.6 $Pa \cdot s^n$), and this value increased when thickener was added (21±6 $Pa \cdot s^n$ and 81±21 $Pa \cdot s^n$ in honey-thick level and pudding-thick level, respectively). By analysing the n and K values for the different thickened samples, all the samples presented similar values at the two levels. The samples thickened with HMP had the lowest K values and the highest n value, while those thickened with GG obtained the lowest n values and the highest K values, especially for the samples at the pudding-thick level.

3.1.2. Viscoelastic analysis

Large amplitude oscillatory shear (LAOS) tests were performed to determine the limits of the linear viscoelastic region (LVR) and the flow point. Figure 2 reflects the changes in elastic modulus, G', and viscous modulus, G'', according to the increasing stress of the thickened pea samples, obtained by the stress sweep test. For all the samples, a low contribution of G'' to the viscoelastic properties of the system was observed. G' was higher than G'' over the entire LVR range, which indicated samples' gel behaviour (Campo-Deaño et al., 2010). After LVR, G' and G'' values decreased with increased stress in all the samples, except for those thickened with GEC and C at the honey-thick

level, and those thickened with NA and NI at the honey and pudding-thick levels. Despite of this, G'' initially increased before lowering again with higher levels of stress. The samples that both moduli decreased with increased stress showed stress thinning behaviour, while the other samples exhibited a weak stress-overshoot behaviour at the onset of the non-linear viscoelastic region (Hyun et al., 2002). Similar behaviour was observed for both the xanthan gum solutions (Carmona et al., 2014) and the pureed carrot thickened with gellan gum, xanthan gum, pectin, carrageenan, and modified corn starch (Sharma et al., 2017). These authors attributed this behaviour not only to the formation of microcracks in the gel structure of these samples, but also to the friction between the rheometer plates at the crack site, which resulted in energy being released and, therefore, in G'' rising.

Table 3 shows the viscoelastic parameters G'_{LVR}, $Strain_{LVR}$, $Stress_{LVR}$ and flow point values, obtained from the LAOS, strain sweep and stress sweep tests.

G'_{LVR} gave an idea of material stiffness (Mezger & Stellrecht, 2000). Of the samples at the honey-thick level, those thickened with CMC, TG, KG and HMP obtained similar and significantly lower G'_{LVR} values ($p<0.05$) than the other samples, which implied the least stiff structure. The samples thickened with C had a significantly higher G'_{LVR} value ($p<0.05$) than the rest, and, thus, greater stiffness. From the samples at pudding-thick level, those thickened with CMC and HMP once again had the least stiff structure, and their G'_{LVR} values were significantly lower ($p<0.05$) than the rest, while the samples thickened with NA presented the greater stiffness with a significantly higher value ($p<0.05$).

$Strain_{LVR}$ and $Stress_{LVR}$ indicated the material's flexibility and elasticity, and can be considered a material stability index (Van Vliet, 2002; Campo-Deaño et al., 2009). The $Strain_{LVR}$ and $Stress_{LVR}$ values for the pea cream were 0.37±0.06 % and 0.41±0.13 Pa,

278 respectively. Table 3 shows that of the samples at the honey-thick level, similar
279 $Strain_{LVR}$ values for the pea cream were observed, except for the samples thickened
280 with NA, NI, XG and HMP that have significantly higher values ($p<0.05$), and those
281 thickened with GEG and C with lower values. These findings can be associated with
282 these samples' greater and lesser flexibility, respectively. The samples thickened with
283 CMC, TG and KG had significant lower $Stress_{LVR}$ values, similarly to the pea cream,
284 while those thickened with C showed a significantly higher value ($p<0.05$) than the rest,
285 which indicated greater elasticity. For the samples at the pudding-thick level,
286 significantly higher values ($p<0.05$) for both parameters were observed in comparison
287 to those for the pea cream. The samples thickened with HMP had the lowest $Strain_{LVR}$
288 and $Stress_{LVR}$ values for both parameters, while those thickened with NI showed the
289 highest values, together with the samples thickened with NA in $Stress_{LVR}$. The highest
290 G'_{LVR} and $Stress_{LVR}$ values, combined with the lowest $Strain_{LVR}$ values of the samples
291 thickened with C, indicated increased brittleness, which could result in a structurally
292 inhomogeneous bolus after chewing the pea cream (Ishihara et al., 2011). Similar results
293 were obtained by Sharma et al. (2017), who worked with thickened carrot purees.
294 The crossover point, where G' = G'' is defined as the flow point, provided information
295 about the breakdown of the internal structure, resulting in the final flow (Mezger, 2006).
296 The samples thickened with XG (at honey-thick level), the samples thickened with NI
297 (at pudding-thick level), and the samples thickened with NA (all the thickened samples)
298 displayed the highest flow point. The samples thickened with CMC, KG and TG (at
299 honey-thick level) and those thickened with HMP (at pudding-thick level) presented the
300 lowest flow point.
301 In order to know the primary structure of the thickened pea creams, a small amplitude
302 oscillatory shear (SAOS) and a creep-recovery test were performed. Figures 3a and 3b

show the frequency sweep curves of G’ of the thickened pea creams obtained with the SAOS test. For all the samples and over the entire frequency range, G’ was higher than G’’, which indicated the samples’ gel behaviour. Moret-Tatay et al. (2015) and Sharma et al. (2017) observed similar behaviours when working with thickened water, milk and juices, and thickened purees, respectively. The dependency of G’ on frequency, using the slope (n’) of log G’ *versus* the log frequency plot can be used as an indicator of gel properties (Yusefi & Rasavi, 2015). True gels have n’ values of 0, dilute solutions have n’ values of 1 or higher, and weak gels take n’ values that fall within the range from 0 to 1. Elastic weak gels have n’ values that come close to 0, while viscous weak gels take n’ values close to 1 (Irani, Razavi, Abdel-Aal, Hucl, & Patterson, 2019). Table 4 shows the n’ values obtained from log G’ *versus* the log frequency plot for all the thickened pea creams. All the values ranged from 0 to 1, which indicated samples’ weak gel behaviour. Samples thickened with NA and NI at both levels, and with C, GEG, and XG at honey-thick level, obtained significantly lower n' values ($p<0.05$) than samples thickened with CMC, TG, KG and HMP at both levels, with more dependence observed on frequency and the highest n' values. The samples thickened with GG had intermediate values. Sharma et al. 2017 also found the highest dependence on frequency for G’ in a carrot puree thickened with CMC compared to other hydrocolloids. Likewise, increased hydrocolloid concentration (from honey-thick to pudding-thick level) seemed to diminish the dependence of G' on frequency with lower n' values and better correlation coefficients than at the honey-thick level, except for the samples thickened with HMP, which showed the same dependence on frequency at both levels.

Figures 3c and 3d depict the frequency sweep curves of the Tan δ values for the thickened pea creams obtained from the SAOS test. Tan δ correlated with both moduli G’ and G’’ (Tan δ = G”/G’) and can be used as a rheological parameter to indicate a

system's physical behaviour. Tan δ values below 0.1 indicate strong gels, Tan δ values above 1 are indicative of dilute solutions, while values between 0.1 and 1 denote weak gels (Ikeda & Nishinari, 2001; Irani et al., 2019). As seen in Figures 3c and 3d, the Tan δ values fell within the 0.1 and 0.6 range, which reinforced the samples' weak gel property. Similar results were observed by Sharma et al., 2017, working with carrot pure thickened with different hydrocolloids. Tan δ can also be used as a rheological criterion to identify bolus that can be safely swallowed by dysphagia patients (Ishihara et al., 2011). This happens when the Tan δ values fall within the 0.1-1 range and G'' is of either the same order of magnitude as, or a lower of an order of magnitude than G'. Of the samples at the honey-thick level, the samples thickened with NA, NI, C and GEG presented a similar tan δ value evolution throughout the frequency range, with low Tan δ values at low frequencies and high ones at high frequencies. The samples thickened with CMC and HMP displayed similar behaviour, with high Tan δ values at low frequencies that increased with frequency. However, despite the results observed in previous samples, tan δ lowered at high frequencies to similar values to the initial ones. The samples thickened with GG, KG and TG seemed to display less dependence on frequency. As Sharma et al. 2017 found, the samples thickened with XG presented a different Tan δ profile to the rest, with values lowering to approximately 10 Hz and then increasing. Of the samples at the pudding-thick level, the samples thickened with NA, NI and HMP showed a similar behaviour to those at the honey-thick level, except for the samples thickened with NI at high frequencies whose Tan δ value sharply dropped. The samples thickened with CMC seemed to show less dependence on frequency, while the samples thickened with GG, KG and TG exhibited much more dependence than at the honey level, with higher Tan δ values at low frequencies that converged at lower values with increasing frequency.

For comparative purposes and for a better interpretation of the results, the viscoelastic parameters obtained from SAOS at 1 Hz are presented in Table 4. As expected for the previous results, G' was higher than G'' for all the samples, and the Tan δ values fell within the 0.1 and 0.6 range, which indicated the samples' weak gel behaviour. The complex modulus (G*) is a measure of material stiffness and rigidity (Mezger, 2006; Payne, Methven, Fairfield, & Bell, 2011), the complex viscosity (η*) is a measure of total resistance to flow according to angular frequency, and the phase angle (δ) measures the difference between the applied deformation and response measured in the material. $\delta = 0^{o}$ depicts perfect elastic, $\delta = 90^{o}$ represents an ideal viscous fluid and δ varies between 0^{o} and 90^{o} for viscoelastic materials. At the honey-thick level, the samples thickened with C and GEG presented the most structural strength in the formed bonds, with significantly higher G ', G * and η * values than for the other samples. The samples thickened with TG, HMP, KG and CMC showed a less rigid structure with significantly lower values ($p<0.05$). At the pudding-thick level, the samples thickened with NA exhibited the most rigid structure, followed by the samples thickened with NI and GG. Those thickened with CMC and HMP had the least rigid structure with significantly lower G', G* and η* values, followed by the samples thickened with TG. Likewise, at the honey level, the samples thickened with NA, NI, C, GEG and XG obtained significantly lower Tan δ and δ values, which denoted the samples' stronger gel behaviour as opposed to the samples thickened with TG with significantly higher values, followed by the samples thickened with KG and HMP displaying weaker gel behaviour. At the pudding level, a similar behaviour to that at the honey level was seen, with significantly lower Tan δ and δ values for the samples thickened with NA and NI, and significantly higher values for the samples thickened with HMP, followed by the samples thickened with TG and KG.

According to Ishihara et al. (2011) and Sharma et al. (2017), a lower Tan δ value and, therefore, greater elastic component contribution, can contribute to increase a material's structural heterogeneity, which can mean that food is more difficult to swallow by reducing, for example, its miscibility with saliva.

Figure 5 shows the variations in creep and recovery compliance J(t) for the thickened pea creams. All the samples exhibited a weak viscoelastic behaviour, as evidenced by a non-linear response to deformation, with the ability to recover some of its structure while eliminating efforts. The maximum J(t) value is related to the samples' internal structure. The samples with high J(t) values have weaker internal structures (Karaman et al., 2012). As expected, a higher hydrocolloid concentration in the samples at the pudding-thick level reinforced the samples' internal structure compared to the samples at the honey-thick level, which obtained lower J(t) values during the analysis. Of the thickened samples, those thickened with HMP, CMC, TG and KG had the highest J(t) values.

The viscoelastic analysis results suggested that the samples thickened with HMP, CMC, TG and KG, which obtained low G' values and high n', Tan δ, and J(t) values at both levels, would have a weaker internal gel structure than the other hydrocolloids, which means an easier bolus to swallow.

3.2. Mastication assay

The normal force *versus* time profiles gave differences in the rheological responses of the pea creams (nectar-thick level) and thickened pea creams at the honey-thick and pudding-thick levels (Figure 5). In each cycle, during compression the maximum force reached at the smallest gap between plates (1 mm) was taken as a measure of sample's "consistency". During decompression, the maximum negative force at the widest

403 distance between plates (3 mm) was related to sample's "adhesiveness". In the fixed gap
404 stage, the recorded apparent shear viscosity (at 10 s^{-1}) was related to the tongue sliding
405 against the palate (Chung et al., 2013).
406 Figure 6 presents the changes in the average values of the maximum positive forces -
407 "consistency" (MF – C), maximum negative force - "adhesiveness" (MF-A) and
408 apparent viscosity according to the number of cycles applied to all the thickened pea
409 creams at both thickened levels, and in the presence/absence of saliva.
410 When saliva was absent, all the measured parameters gradually decreased (although not
411 significantly, $p>0.05$) as the number of cycles increased at both thickened levels. This
412 can be attributed to the progressive breakdown of the material's structure (lower yield
413 stress) in the compression, fixed gap and decompression stages (Chung et al., 2013). At
414 both thickened levels, the samples thickened with CMC showed significantly lower
415 MF-C, while the samples thickened with HMP exhibited the highest MF-C, with no
416 significant differences appearing for the either samples thickened with NA or NI, or
417 those thickened with C, XG and GG at the honey-thick level. The samples thickened
418 with HMP had a significantly higher MF-A than the other samples at both thickened
419 levels, but similar values to those thickened with XG at the honey-thick level and to
420 those thickened with GG at both thickened levels. The samples thickened with GEG,
421 NA, NI, C and CMC at the honey-thick level, and with CMC at the pudding-thick level,
422 had significantly lower MF-A values. The samples thickened with CMC at both the
423 thickened levels obtained the lowest apparent viscosity and significantly differed to the
424 other samples at both thickened levels. At the honey-thick level, the samples thickened
425 with NA obtained the highest apparent viscosity value, but were similar to the samples
426 thickened with C, XG, and GG. At the pudding-thick level, the samples thickened with

NI, GG and KG had the highest apparent viscosity value, followed by the samples thickened with NA and TG.

In the presence of saliva and at both thickened levels, all the parameters decreased in comparison to the samples without saliva, which can be attributed to sample dilution. The strongest effect of saliva on the three studied parameters as the number of cycles increased went to the samples thickened with NA and NI at both thickened levels. This effect was attributed to α-amylase degradation on the starch granules of both samples. This could result in pea creams thickened for dysphagia patients not being safe. According to Ishihara et al. (2011), saliva should function as a binder to form the bolus and as a lubricant for fragmented particles to make the bolus structurally homogeneous and cohesive. Figures 7a and 7b illustrate how the samples thickened with the C profiles with and without saliva being did not significantly differ, which could indicate less miscibility with saliva by generating a non-homogeneous bolus with no lubrication and, therefore, harder to swallow. Viscous components proved to be more miscible with saliva than elastic components. Hence those samples with more viscous components than elastic ones would result easier to swallow.

4. Conclusions

The results of the instrumental tests herein performed confirm that distinct hydrocolloids differ in terms of their viscoelastic and mechanical behaviours regardless of their similar apparent viscosity values at 50 s^{-1} and 25ºC. This allows the structure of foods to be eaten by people with dysphagia problems to be optimised by modifying their viscoelastic balance and making them easier to swallow. In the pea creams with modified textures at the honey-thick and pudding-thick levels, this was achieved by

using the hydrocolloids that provided a higher viscous component, and thus offered greater miscibility with saliva; e.g. samples thickened with CMC, TG and KG.

In order to obtain a complete view of the instrumental behaviour of the studied hydrocolloids, it would be interesting to investigate lubrication properties with tribological tests. This would allow us to understand the behaviour of different hydrocolloids in the oral cavity and, therefore, evaluate their swallowing ease. It would also be interesting to carry out a sensorial study with patients with dysphagia problems, and to evaluate the effect of temperature and storage time on the different properties.

5. Acknowledgments

The authors thank the "Ministerio Español de Ciencia e Innovación" for the financial support provided through the RTI2018-098842-B-I00 Project.

6. References

Abu-Zarim, N., Zainul-Abidin, S. & Ariffin, F. (2018). Rheological studies on the effect of different thickeners in texture-modified chicken *rendang* for individuals with dysphagia. *J Food Sci Technol* 55**,** 4522–4529.

Alvarez, M.D., & Canet W. (2013). Time-Independent and Time-Dependent Rheological Characterization of Vegetable-Based Infant Purees. *Journal of Food Engineering*, *114*, 449–464.

Alvarez, M. D., Fuentes, R., Guerrero, G., & Canet, W. (2017). Characterization of commercial Spanish hummus formulation: Nutritional composition, rheology, and structure. *International Journal of Food Properties*, *20*(4):845-863.

Boehm, M. W., Yakubov, G. E., Stokes, J. R., & Baier, S. K. (2019). The role of saliva in oral processing: Reconsidering the breakdown path paradigm. *Journal of Texture Studies*, https://doi.org/10.1111/jtxs.12411

Campo-Deaño, L., Tovar, C.A., Pombo, M.J., Solas, M.T., & Borderías, A.J. (2009). Rheological study of giant squid surimi (Dosidicus gigas) made by two methods with different cryoprotectants added. *Journal of Food Engineering*, *94*(1), 26-33.

Campo-Deaño, L., Tovar, C.A. & Borderías, A.J. (2010). Effect of several cryoprotectants on the physicochemical and rheological properties of suwari gels from frozen squid surimi made by two methods. *Journal of Food Engineering*, *97*, 457–464.

Carmona, J. A., Ramírez, P., Calero, N., García, M. C., & Muñoz, J. (2014). Non-linear dynamic viscoelasticity of xanthan gum solutions. In P. A. Williams, & G. O. Phillips (Eds.), *Gums and stabilisers for the food industry* 17 (pp. 176-183). Cambridge: Royal Society of Chemistry.

Cepeda, E., García, M.A., Renobales, G. & Costell, E. (2000). Pimento (Capsicum annuum L.) puree: preparation, physicochemical properties and microscopical characterization. *Journal of Food Engineering*, *45*, 85–91.

Cichero, J.A.Y. (2013). Thickening agents used for dysphagia management: effect on bioavailability of water, medication and feelings of satiety. *Nutrition Journal*, *12*(1), 54.

Cichero, J. A., & Murdoch, B. E. (Eds.). (2006). *Dysphagia: foundation, theory and practice*. John Wiley & Sons. Cichero, J.A.Y., Steele, C., Duivestein, J., Clavé, P., Chen, J., Kayashita, J., Dantas, R., Lecko, C., Speyer, R., Lam, P., & Murray, J. (2013). The need for international terminology and definitions for texture-modified foods and thickened liquids used in dysphagia management: foundations of a global initiative. *Current Physical Medicine and Rehabilitation Reports*, *1*(4), 280-291

Cichero, J. A., Lam, P., Steele, C. M., Hanson, B., Chen, J., Dantas, R. O., ... & Pillay, M. (2017). Development of international terminology and definitions for texture-modified foods and thickened fluids used in dysphagia management: the IDDSI framework. *Dysphagia*, *32*(2), 293-314.

Chen, J. (2009). Food oral processing - a review. *Food Hydrocolloids*, *23*(1), 1-25.

Chung, C., Degner, B., & McClements, D. J. (2012). Instrumental mastication assay for textural assessment of semi-solid foods: Combined cyclic squeezing flow and shear viscometry. *Food Research International*, *49*, 161-169.

Chung, C., Olson, K., Degner, B., & McClements, D. J. (2013). Textural Propierties of model food sauces: Correlation between simulated mastication and sensory evaluation methods. *Food Research International, 51*, 310-320.

Dolz, M., González, F., Delegido, J., Hernández, M. J., & Pellicer, J. (2000). A time-dependent expression for thixotropic areas. Application to aerosil 100 hydrogels. *Journal of Pharmaceutical Sciences, 89*, 790–797.

Gallegos, C., Quinchia, L., Ascanio, G., Salinas-Vazquez, M., & Brito-de la Fuente, E. (2012). Rheology and dysphagia: an overview. *Annual Transactions of the Nordic Rheology Society*, *20*, 3-10.

Hanson, B., Cox, B., Kaliviotis, E., & Smith, C.H. (2012a). Effects of saliva on starch thickened drinks with acidic and neutral pH. *Dysphagia, 27*, 427-435.

Hanson, B., O'Leary, M. T., & Smith, C.H. (2012b). The effect of saliva on the viscosity of thickened drinks. *Dysphagia, 27*, 10-19.

Hyun, K., Kim, S. H., Ahn, K. H., & Lee, S. J. (2002). Large amplitude oscillatory shear as a way to classify the complex fluids. *Journal of Non-Newtonian Fluid Mechanics, 107*, 51-65.

Ikeda, S., & Nishinari, K. (2001). “Weak gel”-type rheological properties of aqueous dispersions of non-aggregated k-carrageenan helices. *Journal of Agricultural and Food Chemistry*, 49, 4436-4441.

Irani, M., Razavi, S. M. A., Abdel-Aal, E. S. M., Hucl, P., & Patterson, C. A. (2019). Viscoelastic and textural properties of canary seed starch gels in comparison with wheat starch gel. *International Journal of Biological Macromolecules, 124*, 270–281.

Ishihara, S., Nakauma, M., Funami, T., Odake, S., & Nishinari, K. (2011). Swallowing profiles of food polysaccharide gels in relation to bolus rheology. *Food Hydrocolloids*, *25*(5), 1016-1024.

Jiang, B., Li, W., Hu, X., Wu, J., & Shen, Q. (2015). Rheology of Mung Bean Starch Treated by High Hydrostatic Pressure. *International Journal of Food Properties, 18*, 81–92.

Karaman, S., Yilmaz, M. T., Cankurt, H., Kayacier, A., & Sagdic, O. (2012). Linear creep and recovery analysis of ketchup processed cheese mixtures using mechanical simulation models as a function of temperature and concentration. *Food Research International 48*, 507–519.

Leonard, R. J., White, C., McKenzie, S., & Belafsky, P. C. (2014). Effects of bolus rheology on aspiration in patients with dysphagia. *Journal of the Academy of Nutrition and Dietetics, 114*(4), 590-594.

Mackley, M. R., Tock, C., Anthony, R., Butler, S. A., Chapman, G., & Vadillo, D.C. (2013). The rheology and processing behavior of starch and gum-based dysphagia thickeners. *Journal of Rheology, 57*(6), 1533–1553.

Martino, R., Foley, N., Bhogal, S., Diamant, N., Speechley, M., & Teasell, R. (2005). Dysphagia after stroke: Incidence, diagnosis, and pulmonary complications. *Stroke*, *36*(12), 2756-2763.

548 Mezger, T. G. (2006). *The rheology handbook: for users of rotational and oscillatory*
549 *rheometers*. Vincentz Network GmbH & Co KG. Mezger, T., & Stellrecht, P. (2000).
550 Rheology: The behaviour at rest. *European Coatings Journal, 9*, 18-25.
551 Moret-Tatay, A., Rodríguez-Garcia, J., Martí-Bonmatí, E., Hernando, I., & Hernández,
552 M. J. (2015). Commercial thickeners used by patients with dysphagia: Rheological and
553 structural behaviour in different food matrices. *Food Hydrocolloids, 51*, 318-326.
554 National Dysphagia Diet Task Force & American Dietetic Association.
555 (2002). *National dysphagia diet: Standardization for optimal care*. American Dietetic
556 Associati.
557 Nishinari, K., Takemasa, M., Brenner, T., Su, L., Fang, Y., Hirashima, M., Yosimura,
558 M., Nitta, Y., Moritaka, H., Tomczynska-Mleko, M., Mleko, S, & Michiwaki, Y.
559 (2016). The food colloid principle in the design of elderly food. Journal of Texture
560 Studies, 47, 284-312.
561 Okechukwu, P.E., & Rao, M.A. (1999). Literature values of rheological properties of
562 foods. In Rao, M. A (Ed). *Rheology of Fluid and Semisolid Foods –Principles and*
563 *Applications* (255–317)., Gaithersburg, MD, USA: Aspen publishers.
564 Payne, C., Methven, L., Fairfield, C., & Bell, A. (2011). Consistently inconsistent:
565 commercially available starch-based dysphagia products. *Dysphagia, 26*(1), 27-33.
566 Sharma, M., Kristo, E., Corredig, M., & Duizer, L. (2017). Effect of hydrocolloid type
567 on texture of pureed carrots: Rheological and sensory measures. *Food Hydrocolloids,*
568 *63*, 478-487.
569 Tárrega, A., Durán, L., & Costell, E. (2004). Flow behaviour of semi-solid dairy
570 desserts. Effect if temperature. *International Dairy Journal, 14*(4), 345-353.
571 Torres, O., Yamada, A., Rigby, N. M., Hanawa, T., Kawano, Y., & Sarkar, A. (2019).
572 Gellan gum: A new member in the dysphagia thickener family. *Biotribology, 17*, 8-18.

573 Van Hecke, E., Nguyen, P.U., Clausse, D., & Lanoiselle, J. L. (2012). Flow behaviour
574 of carrot puree: modelling the influence of time, temperature and potato flakes addition.
575 *International Journal of Food Science and Technology, 47*, 177–185.
576 Van Vliet, T. (2002). On the relation between texture perception and fundamental
577 mechanical parameters for liquids and time dependent solids. *Food Quality and*
578 *Preference, 13*(4), 227-236.
579 Yousefi A.R., Razavi S.M.A., Dynamic rheological properties of wheat starch gels as
580 affected by chemical modification and concentration Starch Staerke 2015 567-576
581 Zargaraan, A., Rastmanesh, R., Fadavi, G., Zayeri, F., & Mohammadifar, M. A. (2013).
582 Rheological aspects of dysphagia-oriented food products: a mini review. *Food Science*
583 *Human Wellness, 2*, 173-178.

Table 1. Concentration of added hydrocolloids and final viscosities of the thickened pea creams

Hydrocolloid*	Honey-thick level		Pudding-thick level	
	Concentration (% w/w)	Viscosity (mPas)	Concentration (% w/w)	Viscosity (mPas)
NA	1.35	1534 ± 112	3.2	4171 ± 217
NI	2.15	1572 ± 11	4.8	4152 ± 17
C	3.15	1518 ± 27	-	-
GEG	4.1	1337 ± 27	-	-
XG	0.4	1561 ± 24	-	-
CMC	0.3	1502 ± 63	0.8	4296 ± 85
GG	0.4	1395 ± 46	1.1	4132 ± 269
KG	0.2	1464 ± 73	0.55	4044 ± 50
HMP	1.1	1553 ± 81	2.4	4187 ± 213
TG	0.35	1523 ± 10	0.8	4050 ± 267

Represented data are at a shear rate of $50s^{-1}$ at 25ºC of the thickened pea creams.
Values are the average of two independent experiments.
*NA: Nutavant, NI: Nutilis, C: Carrageenan, GEG: Gellan Gum, XG: Xanthan Gum, CMC: sodium carboxymethylcellulose, GG: Guar Gum, KG: Konjac Gum, HMP: high methoxyl pectin, TG: Tara Gum.

Table 2. Flow rheological behaviour analysis

Hydrocolloid*	Honey-thick level				Pudding-thick level			
	Ar (%)	n	K (Pa·s^n)	R^2	Ar (%)	n	K (Pa·s^n)	R^2
NA	18.6 ± 0.6 ^{a}	0.26 ± 0.02 ^{a}	27 ± 4 ^{a}	0.993	19.3 ± 0.6 ^{a}	0.238 ± 0.009 ^{a}	84 ± 8 ^{a}	0.993
NI	13.9 ± 0.8 ^{bc}	0.287 ± 0.005 ^{ab}	25.7 ± 0.9 ^{a}	0.994	10.0 ± 0.8 ^{b}	0.227 ± 0.004 ^{a}	86 ± 2 ^{a}	0.980
C	17.8 ± 1.3 ^{ab}	0.41 ± 0.02 ^{e}	15.7 ± 1.5 ^{cd}	0.979	-	-	-	-
GEG	9.3 ± 1.5 ^{c}	0.42 ± 0.02 ^{ef}	16.1 ± 1.2 ^{cd}	0.987	-	-	-	-
XG	10.6 ± 0.2 ^{c}	0.26 ± 0.02 ^{a}	28.3 ± 1.4 ^{a}	0.955	-	-	-	-
CMC	13.5 ± 0.4 ^{bc}	0.361 ± 0.002 ^{d}	18.5 ± 0.9 ^{bc}	0.993	9.45 ± 0.96 ^{b}	0.248 ± 0.009 ^{a}	82 ± 1 ^{a}	0.990
GG	2.3 ± 1.4 ^{d}	0.25 ± 0.02 ^{a}	26.1 ± 1.4 ^{a}	0,970	1.88 ± 0.31 ^{e}	0.155 ± 0.001 ^{b}	113 ± 8 ^{b}	0.957
KG	10 ± 2 ^{c}	0.3233 ± 0.004 ^{bc}	21.1 ± 1.2 ^{b}	0.994	6.62 ± 0.18 ^{c}	0.23 ± 0.02 ^{a}	83 ± 7 ^{a}	0.981
HMP	15 ± 3 ^{bc}	0.45 ± 0.03 ^{f}	14 ± 3 ^{d}	0.999		0.451 ± 0.013 ^{c}	36 ± 4 ^{c}	0.996
TG	8.4 ± 1.0 ^{c}	0.335 ± 0.003 ^{cd}	20.8 ± 0.3 ^{b}	0.994		0.230 ± 0.010 ^{a}	83 ± 9 ^{a}	0.979

Values of the thickened pea samples represent Ar: Relative hysteresis area, and the parameters of power law model: n: flow index, K: consistency coefficient, and R^2: correlation coefficient.

Values are the average of two independent experiments.

a-f: Different superscripts indicate significant differences among samples ($p < 0.05$).

*NA: Nutavant, NI: Nutilis, C: Carrageenan, GEG: Gellan Gum, XG: Xanthan Gum, CMC: sodium carboxymethylcellulose, GG: Guar Gum, KG: Konjac Gum, HMP: high methoxyl pectin, TG: Tara Gum.

Table 3. Viscoelastic parameters obtained with the large amplitude oscillatory shear test

	Hydrocolloid*	G'_{LVR} (Pa)	$Strain_{LVR}$ (%)	$Stress_{LVR}$ (Pa)	Flow Point (Pa)
Honey-thick level	NA	547 ± 112^{bc}	0.61 ± 0.03^{cde}	3.38 ± 0.88^{cd}	30.02 ± 4.89^{e}
	NI	455 ± 136^{abc}	0.59 ± 0.25^{bcde}	2.58 ± 0.34^{bc}	19.98 ± 0.40^{d}
	C	1201 ± 508^{d}	0.36 ± 0.06^{ab}	4.55 ± 1.69^{e}	19.46 ± 6.77^{d}
	GEG	719 ± 57^{c}	0.33 ± 0.07^{a}	2.37 ± 0.73^{bc}	10.45 ± 3.45^{c}
	XG	457 ± 24^{abc}	0.64 ± 0.004^{de}	2.98 ± 0.13^{c}	30.90 ± 3.87^{e}
	CMC	93 ± 9^{a}	0.42 ± 0.06^{abcd}	0.44 ± 0.06^{a}	1.91 ± 0.46^{ab}
	GG	275 ± 76^{ab}	0.41 ± 0.07^{abcd}	1.19 ± 0.10^{ab}	10.11 ± 0.51^{bc}
	KG	119 ± 40^{a}	0.44 ± 0.05^{abcd}	0.60 ± 0.24^{a}	3.07 ± 1.41^{ab}
	HMP	174 ± 50^{a}	0.72 ± 0.17^{e}	1.27 ± 0.07^{ab}	12.85 ± 4.28^{cd}
	TG	101 ± 23^{a}	0.41 ± 0.08^{abc}	0.48 ± 0.01^{a}	2.25 ± 0.43^{a}
Pudding-thick level	NA	986 ± 128^{d}	0.99 ± 0.11^{ab}	10.6 ± 1.5^{d}	144 ± 31^{c}
	NI	881 ± 58^{cd}	1.07 ± 0.37^{b}	9.96 ± 4.23^{cd}	94.6 ± 10^{b}
	CMC	318 ± 29^{a}	1.02 ± 0.46^{ab}	3.77 ± 2.03^{ab}	40.2 ± 23^{a}
	GG	808 ± 101^{cd}	0.68 ± 0.10^{ab}	5.88 ± 0.26^{abc}	53.1 ± 6.7^{ab}
	KG	587 ± 7^{bc}	0.68 ± 0.01^{ab}	4.54 ± 0.03^{bcd}	32.2 ± 0.4^{a}
	HMP	252 ± 4^{a}	0.55 ± 0.14^{a}	1.62 ± 0.39^{a}	11.4 ± 2.8^{a}
	TG	709 ± 157^{b}	0.79 ± 0.01^{ab}	6.30 ± 1.31^{ab}	39.7 ± 11^{a}

Viscoelastic parameters represent; elastic modulus value at LVR, G'_{LVR}, strain value at LVR, $Strain_{LVR}$, stress value at LVR, $Stress_{LVR}$, and flow point.

Values are the average of two independent experiments.

a-e: Different superscripts indicate significant differences among samples ($p < 0.05$).

*NA: Nutavant, NI: Nutilis, C: Carrageenan, GEG: Gellan Gum, XG: Xanthan Gum, CMC: sodium carboxymethylcellulose, GG: Guar Gum, KG: Konjac Gum, HMP: high methoxyl pectin, TG: Tara Gum.

Table 4. Slope (n') from Log G' *versus* Log frequency and viscoelastic parameters obtained with the small amplitude oscillatory shear test.

		log G' versus log frequency		Viscoelastic parameters from SAOS test at 1Hz					
	Hydrocolloid*	n'	R^2	η* (Pa s)	G* (Pa)	G'(Pa)	G'' (Pa)	δ (°)	Tan δ
Honey-thick level	NA	0.114 ± 0.004^{a}	0.94 ± 0.06	97 ± 16^{c}	608 ± 98^{c}	603 ± 97^{c}	81 ± 9^{bc}	7.72 ± 0.35^{a}	0.14 ± 0.01^{a}
	NI	0.15 ± 0.01^{a}	0.95 ± 0.04	69 ± 5^{bc}	430 ± 29^{bc}	423 ± 31^{bc}	82 ± 6^{bc}	11.02 ± 1.56^{a}	0.19 ± 0.03^{a}
	C	0.128 ± 0.002^{a}	0.984 ± 0.004	235 ± 55^{e}	1476 ± 344^{e}	1458 ± 338^{e}	233 ± 64^{e}	9.01 ± 0.39^{a}	0.16 ± 0.01^{a}
	GEG	0.12 ± 0.02^{a}	0.978 ± 0.008	171 ± 25^{d}	1077 ± 155^{d}	1064 ± 151^{d}	161 ± 34^{d}	8.56 ± 0.59^{a}	0.15 ± 0.01^{a}
	XG	0.1476 ± 0.0004^{a}	0.970 ± 0.003	75 ± 2^{bc}	473 ± 11^{bc}	463 ± 11^{bc}	96 ± 1^{bc}	11.69 ± 0.08^{a}	0.207 ± 0.002^{a}
	CMC	0.41 ± 0.05^{c}	0.83 ± 0.07	7 ± 3^{a}	44 ± 18^{a}	41 ± 17^{a}	16 ± 4^{a}	22.52 ± 3.45^{bc}	0.42 ± 0.07^{bc}
	GG	0.28 ± 0.04^{b}	0.97 ± 0.02	49 ± 6^{ab}	305 ± 40^{ab}	359 ± 59^{ab}	94 ± 12^{c}	15.04 ± 4.12^{b}	0.27 ± 0.08^{b}
	KG	0.36 ± 0.05^{c}	0.96 ± 0.02	20 ± 1^{a}	125 ± 9^{a}	112 ± 9^{a}	55 ± 2^{abc}	26.31 ± 1.13^{cd}	0.49 ± 0.02^{cd}
	HMP	0.36 ± 0.04^{c}	0.95 ± 0.02	19 ± 3^{a}	119 ± 20^{a}	107 ± 19^{a}	52 ± 5^{ab}	26.27 ± 1.86^{cd}	0.49 ± 0.04^{cd}
	TG	0.38 ± 0.03^{c}	0.98 ± 0.03	21 ± 2^{a}	132 ± 10^{a}	116 ± 7^{a}	64 ± 7^{abc}	28.80 ± 1.34^{d}	0.55 ± 0.03^{d}
Pudding-thick level	NA	0.09 ± 0.01^{a}	0.97 ± 0.01	165 ± 5^{c}	1036 ± 30^{c}	1025 ± 30^{c}	150 ± 3^{a}	8.32 ± 0.08^{a}	0.146 ± 0.002^{a}
	NI	0.160 ± 0.001^{b}	0.982 ± 0.004	$153 \pm 24_{bc}$	1036 ± 30^{c}	937 ± 150^{c}	201 ± 8^{a}	12.23 ± 1.45^{b}	0.22 ± 0.03^{a}
	CMC	0.28 ± 0.03^{cd}	0.991 ± 0.005	66 ± 15^{a}	412 ± 97^{a}	380 ± 94^{a}	160 ± 28^{a}	23.00 ± 1.46^{cd}	0.42 ± 0.03^{bc}
	GG	0.25 ± 0.02^{c}	0.987 ± 0.003	$155 \pm 1_{bc}$	976 ± 4^{c}	912 ± 6^{bc}	350 ± 5^{b}	21.00 ± 0.38^{c}	0.38 ± 0.01^{b}
	KG	0.28 ± 0.03^{cd}	0.982 ± 0.003	145 ± 30^{bc}	912 ± 190^{bc}	831 ± 189^{bc}	375 ± 44^{b}	24.54 ± 2.54^{d}	0.46 ± 0.05^{c}
	HMP	0.359 ± 0.004^{e}	0.991 ± 0.008	46 ± 5^{a}	287 ± 33^{a}	244 ± 33^{a}	151 ± 10^{a}	31.75 ± 1.76^{e}	0.62 ± 0.04^{d}
	TG	0.2984 ± 0.0006^{cd}	0.984 ± 0.004	123 ± 6^{b}	776 ± 37^{b}	700 ± 28^{b}	333 ± 27^{b}	25.43 ± 0.87^{d}	0.48 ± 0.02^{c}

Viscoelastic parameters represent; η*: complex viscosity, G*: complex modulus, G´: elastic modulus, G´´: viscous modulus, δ: phase angle, and Tan δ: loss tangent.

Represented data are at 1Hz and values are the average of two independent experiments.

a-e: Different superscripts indicate significant differences among samples ($p < 0.05$).

*NA: Nutavant, NI: Nutilis, C: Carrageenan, GEG: Gellan Gum, XG: Xanthan Gum, CMC: sodium carboxymethylcellulose, GG: Guar Gum, KG: Konjac Gum, HMP: high methoxyl pectin, TG: Tara Gum.

Figure captions

Figure 1. Typical flow curve for the pea cream and thickened pea creams

Figure 2. Changes in elastic modulus, G' (a and c), and viscous modulus, G'' (b and d) according to stress for the thickened pea samples (NA: Nutavant, NI: Nutilis, C: Carrageenan, GEG: Gellan Gum, XG: Xanthan Gum, CMC: sodium carboxymethylcellulose, GG: Guar Gum, KG: Konjac Gum, HMP: high methoxyl pectin, TG: Tara Gum). Curves are representative runs.

Figure 3. Frequency sweep curves of elastic modulus, G' (a and b) and loss tangent, Tan δ (c and d) of the thickened pea creams (NA: Nutavant, NI: Nutilis, C: Carrageenan, GEG: Gellan Gum, XG: Xanthan Gum, CMC: sodium carboxymethylcellulose, GG: Guar Gum, KG: Konjac Gum, HMP: high methoxyl pectin, TG: Tara Gum). Curves are representative runs

Figure 4. Variation of the creep and recovery compliance J(t) data with increasing applied shear stress for all the thickened pea creams (NA: Nutavant, NI: Nutilis, C: Carrageenan, GEG: Gellan Gum, XG: Xanthan Gum, CMC: sodium carboxymethylcellulose, GG: Guar Gum, KG: Konjac Gum, HMP: high methoxyl pectin, TG: Tara Gum). Curves are representative runs

Figure 5. Mastication profile of the pea creams at the nectar-thick, honey-thick and pudding-thick levels.

Figure 6. Changes in maximum positive force - “consistency” and maximum negative force “adhesiveness” during cycles of the pea creams (NA: Nutavant, NI: Nutilis, C: Carrageenan, GEG: Gellan Gum, XG: Xanthan Gum, CMC: sodium carboxymethylcellulose, GG: Guar Gum, KG: Konjac Gum, HMP: high methoxyl pectin, TG: Tara Gum): a) Honey-thick level without saliva; b) Honey-thick level with saliva; c) Pudding-thick level without saliva; d) Pudding-thick level with saliva.

Figure 7. Changes in apparent viscosity at $10s^{-1}$ (mPas) during cycles of the pea creams (NA: Nutavant, NI: Nutilis, C: Carrageenan, GEG: Gellan Gum, XG: Xanthan Gum, CMC: sodium carboxymethylcellulose, GG: Guar Gum, KG: Konjac Gum, HMP: high methoxyl pectin, TG: Tara Gum): a) Honey-thick level without saliva; b) Honey-thick level with saliva; c) Pudding-thick level without saliva; d) Pudding-thick level with saliva.

Figure 1

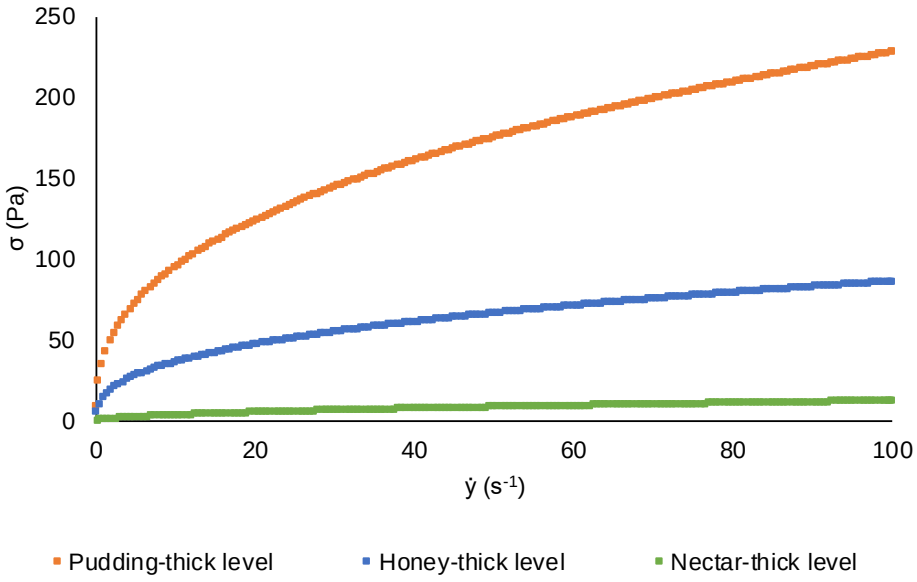
250
200
150
100
50
0
σ (Pa)
0
20
40
60
80
100
γ̇ (s-1)
Pudding-thick level
Honey-thick level
Nectar-thick level

Figure 2

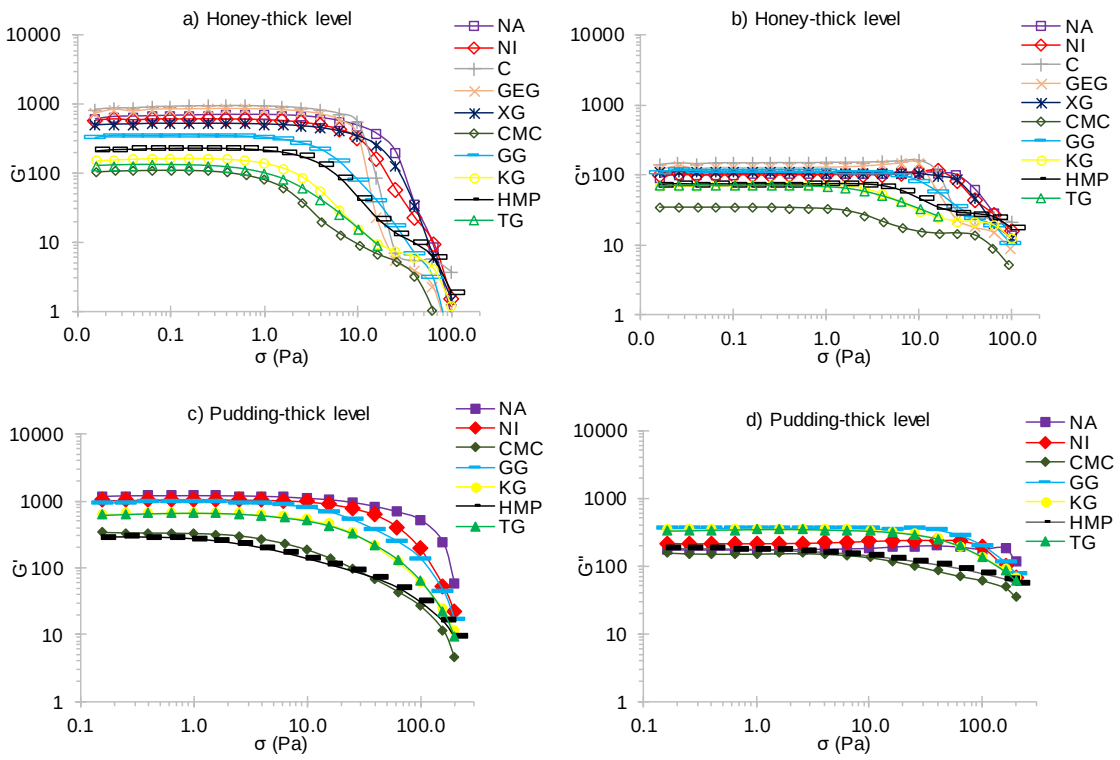
a) Honey-thick level
b) Honey-thick level
c) Pudding-thick level
d) Pudding-thick level
NA
NI
C
GEG
XG
CMC
GG
KG
HMP
TG
10000
1000
100
10
1
0.0
0.1
1.0
10.0
100.0
σ (Pa)

Figure 3

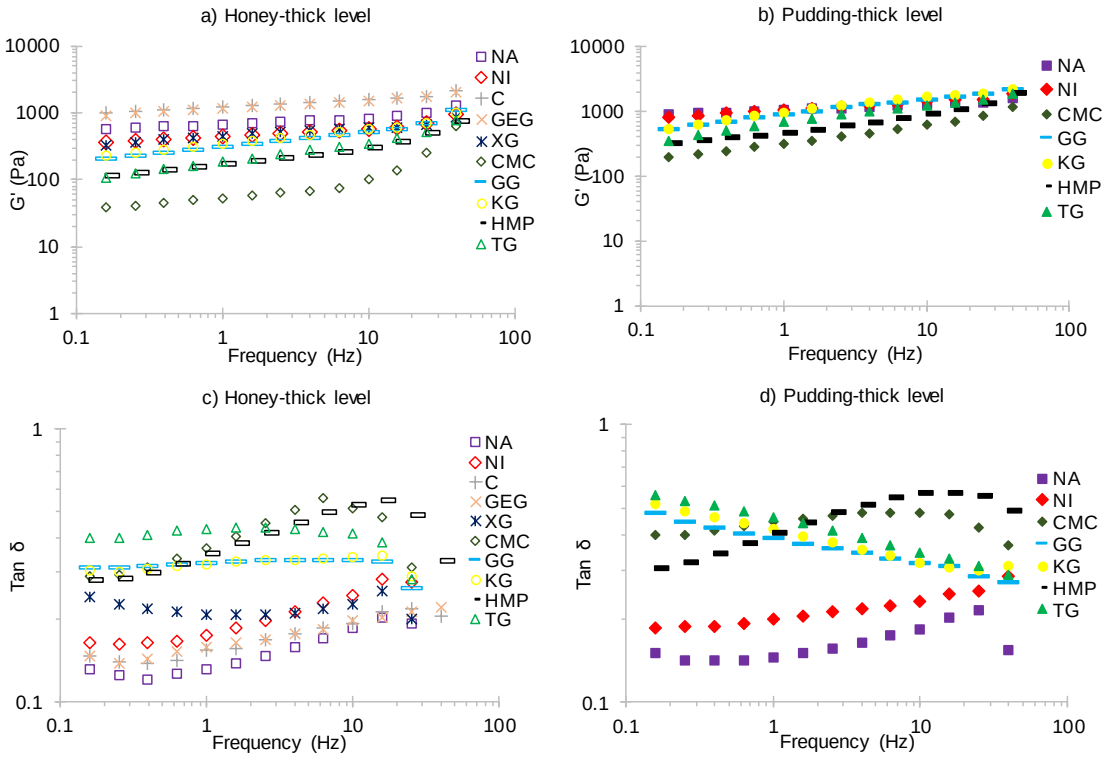
a) Honey-thick level
G' (Pa)
Frequency (Hz)
NA
NI
C
GEG
XG
CMC
GG
KG
HMP
TG
b) Pudding-thick level
G' (Pa)
Frequency (Hz)
NA
NI
CMC
GG
KG
HMP
TG
c) Honey-thick level
Tan δ
Frequency (Hz)
NA
NI
C
GEG
XG
CMC
GG
KG
HMP
TG
d) Pudding-thick level
Tan δ
Frequency (Hz)
NA
NI
CMC
GG
KG
HMP
TG

Figure 4

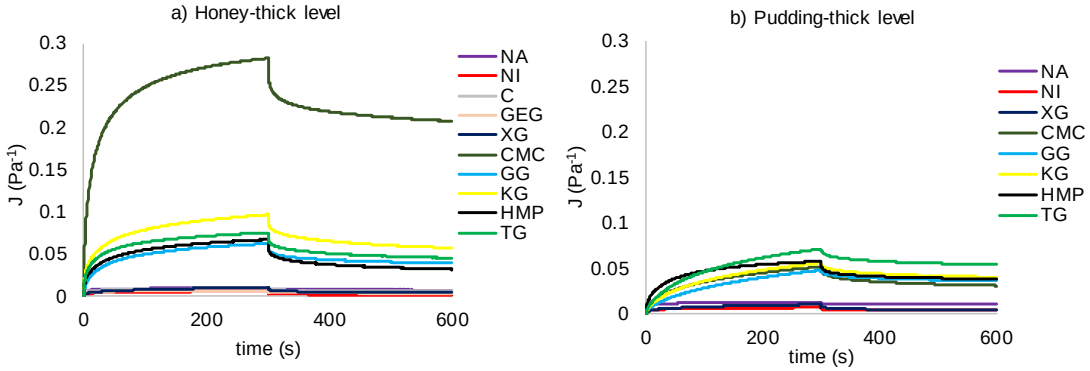
a) Honey-thick level
J (Pa-1)
0.3
0.25
0.2
0.15
0.1
0.05
0
0
200
400
600
time (s)
NA
NI
C
GEG
XG
CMC
GG
KG
HMP
TG
b) Pudding-thick level
J (Pa-1)
0.3
0.25
0.2
0.15
0.1
0.05
0
0
200
400
600
time (s)
NA
NI
XG
CMC
GG
KG
HMP
TG

Figure 5

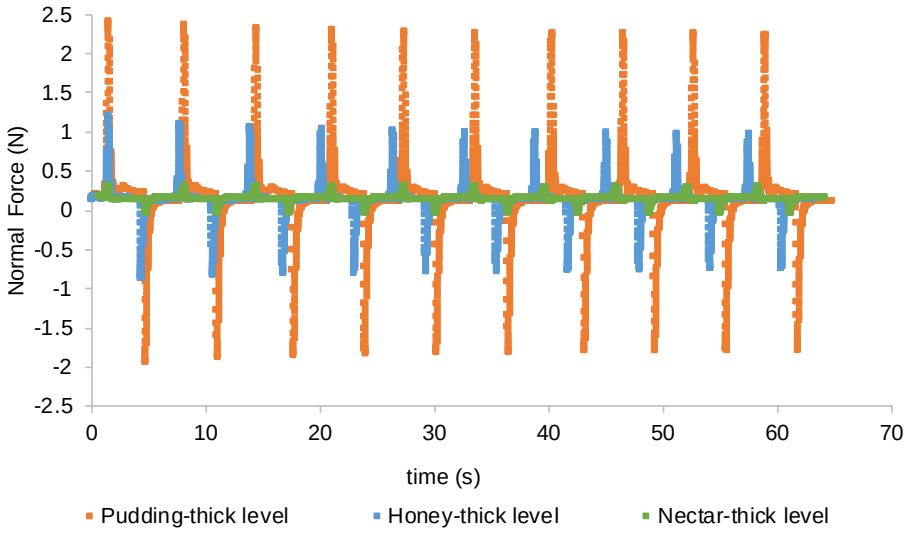
2.5
2
1.5
1
0.5
0
-0.5
-1
-1.5
-2
-2.5
Normal Force (N)
0
10
20
30
40
50
60
70
time (s)
Pudding-thick level
Honey-thick level
Nectar-thick level

Figure 6

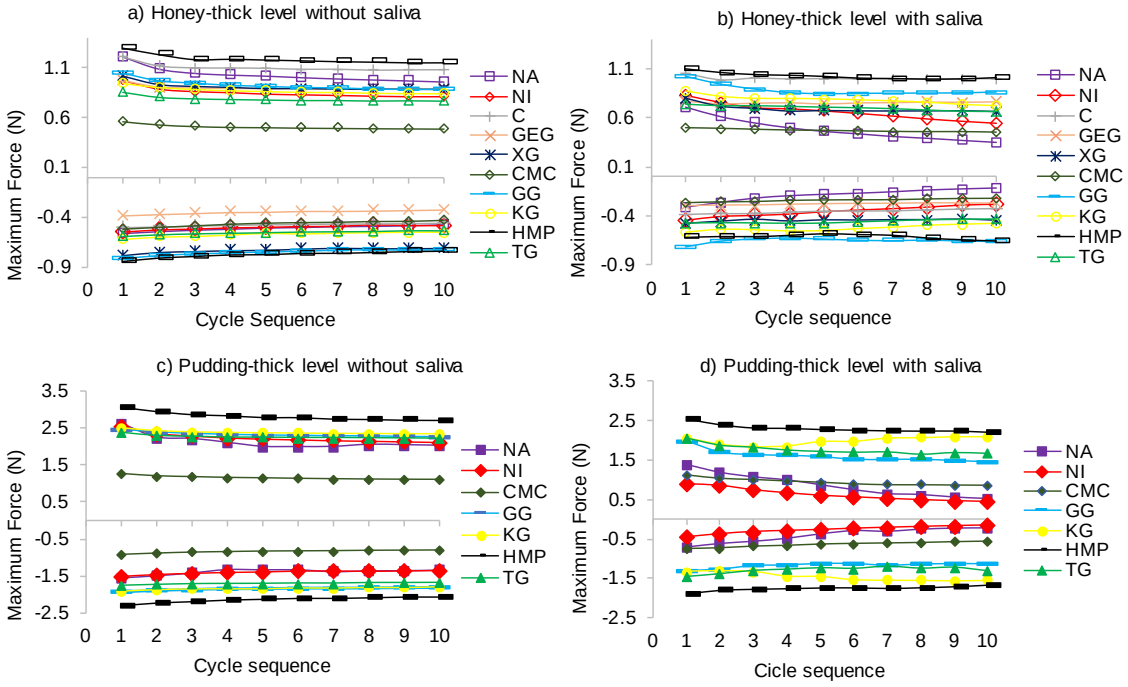
a) Honey-thick level without saliva
Maximum Force (N)
1.1
0.6
0.1
-0.4
-0.9
0 1 2 3 4 5 6 7 8 9 10
Cycle Sequence
NA
NI
C
GEG
XG
CMC
GG
KG
HMP
TG
b) Honey-thick level with saliva
Maximum Force (N)
Cycle sequence
c) Pudding-thick level without saliva
3.5
2.5
1.5
0.5
-0.5
-1.5
-2.5
Cycle sequence
d) Pudding-thick level with saliva
Cicle sequence

Figure 7

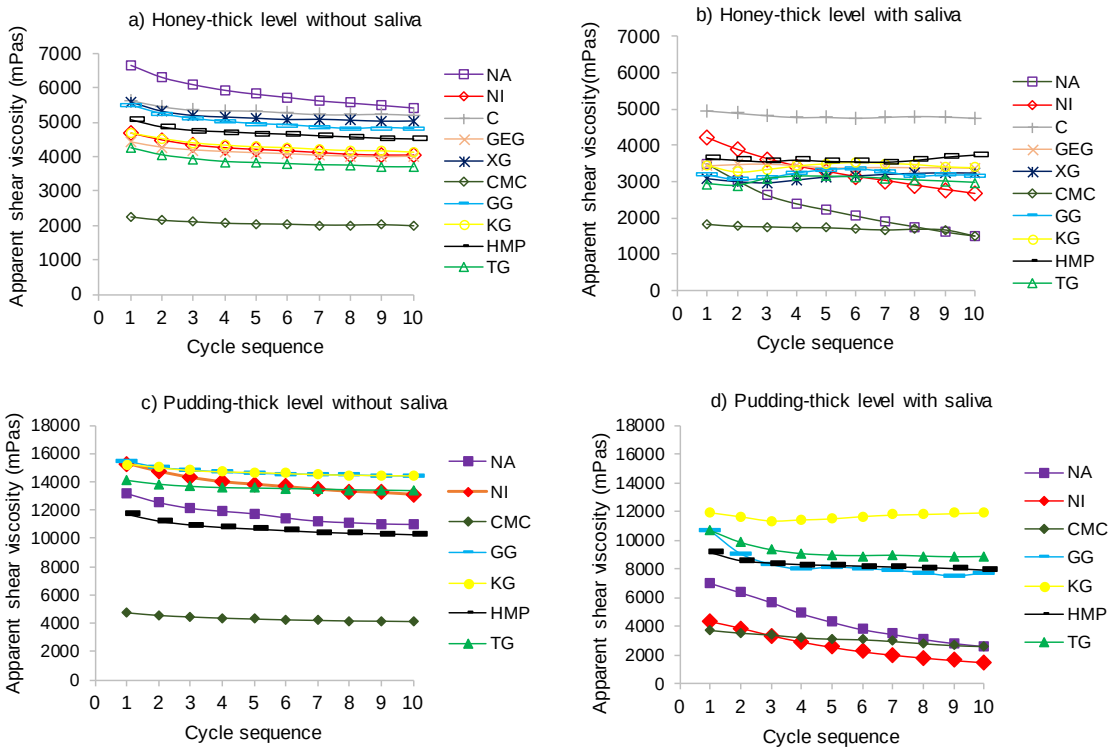
a) Honey-thick level without saliva
Apparent shear viscosity (mPas)
Cycle sequence
NA
NI
C
GEG
XG
CMC
GG
KG
HMP
TG
b) Honey-thick level with saliva
Apparent shear viscosity(mPas)
Cycle sequence
c) Pudding-thick level without saliva
Apparent shear viscosity (mPas)
Cycle sequence
d) Pudding-thick level with saliva
Apparent shear viscosity (mPas)
Cycle sequence